promoting access to White Rose research papers

White Rose Research Online

Universities of Leeds, Sheffield and York
http://eprints.whiterose.ac.uk/

This is the author's version of an article published in the **International Journal of Hydrogen Energy**

White Rose Research Online URL for this paper:

http://eprints.whiterose.ac.uk/id/eprint/75954

Published article:

Zin, RM, Lea-Langton, A, Dupont, V and Twigg, MV (2012) *High hydrogen yield and purity from palm empty fruit bunch and pine pyrolysis oils.* International Journal of Hydrogen Energy, 37 (14). 10627 - 10638. ISSN 0360-3199

http://dx.doi.org/10.1016/j.ijhydene.2012.04.064

White Rose Research Online
eprints@whiterose.ac.uk

High hydrogen yield and purity from palm empty fruit bunch and pine pyrolysis oils

Authors

Rohaya Md Zin[1], Amanda Lea-Langton[1], Valerie Dupont[1], Martyn V. Twigg[2]

[1]*Energy Research Institute, The University of Leeds, Leeds LS2 9JT, UK*

[2]*Johnson Matthey Orchard Laboratory, Orchard Road, Royston, SG8 5HE, UK*

Corresponding author:

Valerie Dupont

Energy Research Institute,
Energy Building,
The University of Leeds,
LS2 9JT
United Kingdom

Email V.Dupont@leeds.ac.uk

Tel: (00 44) 113 3432503 outside UK
0113 3432503 inside UK

Fax: (00 44) 113 246 7310

Paper accepted in International Journal of Hydrogen Energy

Published article reference:

Md Zin, R., Lea-Langton, A., Dupont, V., Twigg, M.V., 2012. High hydrogen yield and purity from palm empty fruit bunch and pine pyrolysis oils. International Journal of hydrogen energy 37 (2012) 10627-10638

High hydrogen yield and purity from palm empty fruit bunch and pine pyrolysis oils

Rohaya Md Zin[1], Amanda Lea-Langton[1], Valerie Dupont[1]*, Martyn V. Twigg[2]

[1]*Energy Research Institute, The University of Leeds, Leeds LS2 9JT, UK*

[2]*Johnson Matthey Orchard Laboratory, Orchard Road, Royston, SG8 5HE, UK*

Abstract

The benefits of CO_2 sorption enhanced steam reforming using calcined dolomite were demonstrated for the production of hydrogen from highly oxygenated pyrolysis oils of the agricultural waste palm empty fruit bunches (PEFB) and pine wood. At 1 atm in a down-flow packed bed reactor at 600 °C, the best molar steam to carbon ratios were between 2 and 3 using a Ni catalyst. After incorporating steam-activated calcined dolomite as the CO_2 sorbent in the reactor bed, the H_2 yield from the moisture free PEFB oil increased from 9.5 to 10.4 wt% while that of the pine oil increased from 9.9 to 13.9 wt%. The hydrogen purity also rose from 68 to 96% and from 54 to 87 % for the PEFB and pine oils respectively, demonstrating very substantial sorption enhancement effects.

Keywords: steam reforming, CO_2-sorption enhancement, pyrolysis oil, nickel catalyst, hydrogen production, dolomite

1. Introduction

Fossil fuels contribute to more than 90% of the world hydrogen production. Depletion of resources and environmental issues related to high CO_2 emissions and climate change, as well as air pollution will make fossil fuels' availability and consumption less dominant in the future. The situation has led to significant research on the production of hydrogen from renewable energy including waste biomass.

Steam reforming of pyrolysis oils has received considerable attention from various research groups [1, 2], [3-5] and [6-8] for the past years. Results from the studies have confirmed that pyrolysis oils comprise complex mixtures of oxygenates that can be steam reformed to produce hydrogen.

Studies on steam reforming of pyrolysis oils and their aqueous fraction have been carried out using representative compounds such as acetic acid, acetone, ethylene glycol and ethanol. Acetic acid, one of major constituents of pyrolysis oil that can reach up to 12 wt% of biomass oils [9], has become the focus of research in steam reforming [10],[11] [12] [13] [1] [14, 15] [16]. Vagia and Lemonidou [7] reported that the yield of H_2 approached 80% of the maximum when steam reforming acetic acid at 750 °C, producing mainly H_2, CO_2 and CO, and small amount of CH_4 . Steam reforming of acetic acid at lower temperatures than 750 °C has been found to lead to carbonaceous deposits on the catalysts bed. Temperatures above 600 °C and molar steam to carbon ratios (S/C) above 3 were reported to be ideal conditions for complete reforming of model compound mixtures (acetic acid, acetone, ethylene glycol) [17]. Boudouard and thermal decomposition reactions may contribute to the formation of carbon deposits. Results from studies on steam reforming using the aqueous phase of pyrolysis oils (obtained by phase separation after addition of water to the pyrolysis oil) revealed that the coke deposits on catalysts have a polyaromatic structure, in contrast to those

produced by model compounds, which had a graphitic nature [17] . Catalyst deactivation due to carbon deposition is one of major challenges in the steam reforming of pyrolysis oil, which has major effects on the process performance by decreasing the desirable products CO_2 and H_2 and increasing the undesirable products CO and CH_4. Many studies related to steam reforming of pyrolysis oils and model compounds employ Ni-based catalyst as the reforming catalyst [2, 3, 18-21].

Results from the catalytic steam reforming and from early cycles of the chemical looping reforming of pyrolysis oil derived from palm empty fruit bunches (PEFB) and pinewood have been published by the authors [22]. PEFB is a by-product generated during the fruit stripping stage at the oil mill processing plant. Malaysia is the world second largest producer of palm oil [23, 24] and can be considered as the major producer of PEFB based on the assumption that a kg of palm oil generates a kg of wet PEFB [25]. In the present study, PEFB and pine wood pyrolysis oils were steam-reformed to produce high purity hydrogen using the process of sorption-enhancement. A mixture of calcined dolomite and of nickel catalyst was used in this study.

This study aims to investigate the feasibility of firstly, sorption enhanced steam reforming PEFB and pine oils, and secondly, quantifying the effects of sorption-enhancement via the increases in both H_2 yield and H_2 purity achieved in the presence of a Ca-based sorbent. Comparisons are drawn with the thermodynamic equilibrium calculations for the sorption enhancement of the major components measured in the bio-oils.

2. Materials and Methods

2.1. Materials

2.1.1. Characterisation of the oils

The pyrolysis oils were purchased from BTG, Netherlands where they were produced using a non-catalytic fast pyrolysis process. They were filtered to remove fibrous material to prevent clogging of the fuel delivery lines. Characteristics of these oils are reported elsewhere (Lea-Langton et al., 2011), including density, pH, gross calorific value (bomb calorimetry), water content (Karl Fischer titration), C/H/N/O elemental analysis, and inorganics content (K, S, Ca, Si, Fe, Al, Mg, P, Na, Br) by ICP-MS, volatiles, carbonaceous residue, ash content and thermal decomposition kinetics were obtained from TGA measurements. To summarise, both oils were acidic (pH ≤ 3.2), had low gross calorific value (≤15 MJ kg^{-1}), high carbonaceous residue (~11wt%) and high ash content (~3 wt%), with significant S, Ca and Si impurities (~500 ppm). In particular PEFB oil had a high K content (1418 ppm), and pine oil a significant Fe content (620 ppm). This resulted in the molar formulae of $C_{0.1845}H_{0.4873}O_{0.3233}N_{0.0049}$ for the 'wet' PEFB oil, and $C_{0.2462}H_{0.5024}O_{0.2502}N_{0.0012}$ for 'wet' pine oil. Using the measured water contents of 32 and 22 wt% for PEFB and pine oils respectively, a moisture-free (m.f.) molar formula was then be derived for each oil via elemental balances, resulting in $C_{0.3178}H_{0.3605}O_{0.3132}N_{0.0085}$ for the m.f. PEFB oil, and $C_{0.3372}H_{0.4440}O_{0.2171}N_{0.0017}$ for the m.f. pine oil.

The organic compounds in the filtered pyrolysis oils were identified using an Agilent 5975B inert XLMSD gas chromatography-mass spectrometry (GS-MS) unit equipped with slightly polar capillary column Restek Rtx 1701 and MS detector. The initial temperature of the oven was 60 °C and held for 2 minutes before increasing to final temperature of 280 °C at 5 °C/min heating rate. The final temperature was held for 20 minutes. Helium was used as the carrier gas and solvent delay time was set at 6 minutes. All samples of pyrolysis oils were prepared by dissolving it in methanol.

It is not possible to 'dry' the oils without losing a significant portion of their volatiles content, therefore the oils can only be used in their 'wet' state. However, knowledge of the moisture

free molar elemental composition of the oils allows the calculation of maximum H_2 yields, the stoichiometric S/C ratio, maximum water conversions and water flow rate to achieve a specific S/C ratio in the experiments. E.g, the stoichiometric S/C ratios were, based on moisture free compositions, 1.01 and 1.36 for the PEFB and pine oils, respectively. Similarly, the maximum H_2 yields were 10.9 wt % and 17.1 wt% of the m.f. PEFB and pine oils respectively. For the PEFB oil, 36% of this maximum hydrogen yield would originate from the oil and 64% from the water co-reactant. For pine oil, the maximum hydrogen yield had a 32.5% oil and 67.5% water contributions. In comparison, the maximum H_2 yield from SR-WGS of acetic acid is 13.3 wt%, with a 50/50 % split between fuel and water contributions.

Comparisons of experimental outputs with model compounds in similar steam reforming conditions can then be performed.

2.1.2. Solids characterisation

The catalyst was originally supplied in pellet form (Johnson Matthey Plc) and consisted of 18 wt% NiO on a crystalline alpha-alumina support when fully oxidized, as per its MSDS. Nickel is widely considered as the most suitable metal for steam reforming of hydrocarbons [26]. The surface area of the catalyst was measured by the BET method with a Quantachrome Instrument Nova® 2200. The catalyst had relatively low surface area (2.3 $m^2 g^{-1}$). Imaging and analysis of the catalyst's surface before and after steam reforming were performed by TEM coupled with EDX. The equipment used was a FEI CM200 field emission gun (FEG) TEM running at 197 kV equipped with an Oxford Instruments energy dispersive X-ray (EDX) spectrometer and a Gatan Imaging Filter. The images of the as-received catalyst revealed a very crystalline Al_2O_3 support with NiO particle deposits of around 50 nm size. The catalyst's composition of 17.9 wt% NiO on α-Al_2O_3 was confirmed using Rietveld

refinement [27] of the powder XRD spectra obtained from the as-received catalyst ground to a fine powder. The XRD apparatus was a X'pert MPD by PANalytical, fitted with a Cu-K anode, and used in the range of angles from 2θ= 5º to 2θ= 90º at increments of 0.017º, with a scan step time of 40.7 s. The Highscore Plus software was used for peak fitting and analysis of the diffractograms in the Rietveld refinement and for the calculation of crystallite sizes following the Scherrer equation corrected for peak broadening caused by instrumentation and strain. The crystallites of NiO were measured at 44.7 nm for the as-received catalysts. Crystal size and phase composition of the catalyst after the steam reforming experiments was also performed.

The dolomite CO_2 sorbent was supplied as granules (3- 4 mm) by WBB minerals (Warmsworth Quarry, South Yorkshire, England) and contained 21.3 wt.% MgO, 30.7 wt.% CaO, 0.3 wt.% SiO_2, 0.27 wt.% Fe_2O_3, and 0.1 wt.% Al_2O_3 and 47.33 wt% CO_2.

Dolomite is a natural mineral containing near equimolar amounts of magnesium and calcium carbonate. After calcination, only the calcium oxide component is able to re-carbonate while MgO remains chemically inert [28, 29]. Other compounds are finely dispersed in small crystallites on dolomite [30]. Earlier studies [31] showed that using a mixture of reforming catalyst and CaO (derived from calcinations of high-purity $CaCO_3$) in a single reactor, high H_2 concentration of >95% could be achieved. CaO-based sorbents combine well with bio-oil steam reforming because of their high capacity and fast kinetics at the temperatures of maximum hydrogen yield (500-700°C), when temperatures in excess of 600°C have been shown necessary to ensure significant bio-oils conversion in practice [17]. The inexpensive dolomite was chosen over limestone in many studies on the basis that it gives better multicycle performance [32-35]. The methane SESR experiment by Lopez-Ortiz and Harrison [36] exhibited only moderate activity loss after twenty cycles of carbonation-calcination of a pre-treated dolomite with a commercial Ni-based catalyst. These studies have

focused on methane fuel for this process, but other feedstock that have successfully been tested for the sorption-enhanced steam reforming process are crude glycerol and vegetable waste cooking oil. Hydrogen purities above 90% with low concentration of CO_2 have been obtained during sorbent pre-saturation conditions when steam reforming crude glycerol and waste cooking oil in the presence of calcined dolomite [37-39]. The authors have studied the cyclic carbonations and thermal decompositions of dolomite at the micro-reactor and bench reactor scales [40]. The effects of partial pressure of CO_2 and of H_2O on the kinetics of the global reactions were investigated, revealing significant increases in carbonation capacity in the presence of relatively small partial pressures of H_2O.

2.2. Reactor setup

The schematic diagram of the steam reforming equipment setup is presented in Fig. 1. The reactor incorporated a down-flow quartz reactor of 12 mm ID and 70 cm long. The reactor was held inside a tube furnace. MKS mass flow controllers were used to control the gas flow rates (N_2, H_2 and air). Two programmable syringe pumps by New Era Pump Systems provided separate PEFB oil and water liquid flows. The reactor's off-gas was cooled via two condenser units and the moisture was removed by a silica gel trap prior to entering the gas analyzers. ABB analysers were used to record online hydrogen, methane and carbon oxide products respectively at 5 s intervals. H_2 was measured by a thermal conductivity detector (Caldos 15) and CO, CO_2 and CH_4 via non-dispersive infra-red absorption-based instruments (Uras 14).

2.3. Experimental procedures for steam reforming

The catalyst and dolomite were crushed separately and sieved to 0.85 – 2 mm size particles. The size of the dolomite particles was the same as the catalysts particles so as to avoid altering the flow patterns in the reactor bed when comparing conditions with and without sorbent. The size for the catalyst was optimally chosen to prevent large pressure drop (too small particles) and diffusion limitations caused by too large particles. Nevertheless mass transfer effects are expected in the current system as they would be in a scaled up version. The same amount (6.0 g) of catalyst was used for all experimental runs, mixed with steam-activated calcined dolomite (6.0 g) for the sorption enhanced experiments. For the steam activation procedure, ground dolomite was loaded on its own into the reactor. Water was fed into the reactor with a heating rate and set temperature of 850 °C (1.583 cm^3 min^{-1}) together with N_2 (200 cm^3 min^{-1}, STP). Initially the release of CO_2 increased with temperature until it reached a maximum, at a furnace temperature of 800 °C, then it slowly decreased to zero, indicating the end of the decarbonation (calcination) reaction. The furnace was then switched off and allowed to cool overnight. After discharging the activated dolomite, the reactor was re-loaded with a mixture of catalyst and steam activated calcined dolomite.

The steam reforming experiments were carried out at atmospheric pressure and 600 °C with varying molar S/C ratios without sorbent, and after identification of the optimal S/C ratio, the experiments were repeated with sorbent. The experiments began with reduction of the catalyst to convert all the NiO to the active phase of Ni. This step used nitrogen and hydrogen flow rates of 200 and 10 cm^3 min^{-1} (STP), respectively. The H_2 flow was stopped keeping just the N_2 and injection of the 'wet' pyrolysis oil and water began using the two programmable syringe pumps. Experiments were ended by switching off first the fuel and then water flows, leaving the N_2 gas flow on, still at 600 °C, and when the reformate gases concentrations had subsided, N_2 flow was also turned off. Finally the catalyst was reoxidised, also burning-off

any carbon that may have been formed on the catalyst, in a flow of air (500 cm^3 min^{-1}, STP) at a set temperature of 600 °C for the experiments without sorbent, and 970 cm^3 min^{-1} (STP) at 850 °C for those with sorbent (the higher temperature was used to calcine the sorbent). The release of CO and CO_2 was monitored by the on-line analyser to complete the carbon and oxygen balances. Typically during air feeds with and without sorbent, the recorded temperature increased by 10-15 °C caused by the oxidation reactions of the carbon residue and the reoxidation of the nickel catalyst. The flow of 200 N_2 cm^3 min^{-1} (STP) was maintained throughout the steam reforming stage to enable calculation through material balances of the fuel and steam conversions, H_2 yield and selectivity to H-containing and C-containing products as outlined below using Eqs 1-4. The analysers measured the exit dry gas concentrations and mol (vol) fractions 'y_i' of CH_4, CO, CO_2, O_2 and H_2 were calculated. The mol fraction of nitrogen, y_{N_2} was calculated by balance to 1. The total dry molar flow rate leaving the reactor $\dot{n}_{out,dry}$ was determined via a nitrogen balance.

The ideal process outputs from sorption enhanced steam reforming provide a basis for comparison of the real process. The steam reforming reactions of an organic fuel followed by water gas shift ('SR' and 'WGS') and the principle behind sorption enhancement with a Ca-based CO_2 sorbent via its carbonation ('CB') are given in the following equations:

$$C_nH_mO_k + (n\text{-}k)H_2O \leftrightarrow nCO + (n+0.5m\text{-}k)H_2 \qquad \text{SR}$$

$$CO + H_2O \leftrightarrow CO_2 + H_2 \qquad \text{WGS}$$

$$CaO_{(S)} + CO_2 \leftrightarrow CaCO_{3(S)} \qquad \text{CB}$$

The carbonation reaction removes CO_2 from the reformate gases and thus promotes a favourable shift in the WGS equilibrium, which has the triple effect of increasing the H_2 concentration (effectively resulting in higher H_2 purity), increasing the H_2 production yield, and decreasing the temperature of maximum H_2 yield. According to the stoichiometry of the

complete SR and WGS reactions, this maximum is (2*n*+0.5*m*-*k*) mol of H_2 per mol of $C_nH_mO_k$ fuel, or, when reported in wt% of the fuel, 100×2.02×(2*n*+0.5*m*-*k*)/(12.01*n*+1.01*m*+16*k*). This is superior to the maximum that would be reached under the thermodynamic equilibrium limited reactions without sorption enhancement, as the reverse WGS reaction prevents complete CO conversion to CO_2. However, regeneration of the Ca-based CO_2 sorbent by temperature swing represents an energy penalty of the sorption enhanced steam reforming process, but costs can be minimised by process intensification measures such as chemical looping reforming, as explored in detail with waste cooking oil as feedstock [38].

A carbon balance yields the oil conversion fraction X_{oil} to the main C-containing products (CH_4, CO, CO_2) according to (1).

$$X_{oil} = \frac{\dot{n}_{out,dry}\left(y_{CH_4} + y_{CO} + y_{CO_2}\right)}{n \times \dot{n}_{oil,in}} \qquad (1)$$

Where *n* was the moles of atomic C in the moisture free (m.f.) oil elemental molar formula. A hydrogen balance yielded an estimate of the fractional steam conversion, equation (2), in which

$$X_{H_2O} = \frac{1}{\dot{n}_{H_2O,in}} \times \left[\dot{n}_{out,dry}\left(2y_{CH_4} + y_{H_2}\right) - 0.5m\left(\dot{n}_{oil,in}X_{oil}\right)\right] \qquad (2)$$

m was the moles of atomic H in the m.f. oil. The H_2 purity '*H_2 pur*' and the hydrogen yield '*H_2 yield*' were defined as in equation (3) and (4) respectively:

$$H_2\,pur = 100 \times \frac{y_{H_2}}{\left(y_{H_2} + y_{CO_2} + y_{CO} + y_{CH_4}\right)} \qquad (3)$$

$$H_2\ \text{yield} = 100 \times \frac{W_{H_2} \times y_{H_2} \times \dot{n}_{out,dry}}{W_{oil} \times \dot{n}_{oil,in}}\ \text{wt\% of oil (m.f.)} \qquad (4)$$

Where *W* is the relevant molar mass concerned.

The H_2 yield efficiency or 'H_2 eff' is the ratio (in %) of H_2 yield during the experiments to the theoretical stoichiometric maximum H_2 yield (Eq. 5).

The selectivity to the C-containing products ('*Sel*') was defined according to Eqs. 6-8:

$$SelCO_2 = 100 \times \frac{y_{CO_2}}{\left(y_{CO_2} + y_{CO} + y_{CH_4}\right)} \quad (6);$$

$$SelCO = 100 \times \frac{y_{CO}}{\left(y_{CO_2} + y_{CO} + y_{CH_4}\right)} \quad (7);$$

$$SelCH_4 = 100 \times \frac{y_{CH_4}}{\left(y_{CO_2} + y_{CO} + y_{CH_4}\right)} \quad (8)$$

To provide a measure of the combined steam reforming and water gas shift efficiency, the output parameters for a given experiment are compared with their ideal theoretical counterparts notwithstanding equilibrium limitations (see end section 2.1.1).

Moreover, when comparing the process outputs with and without CaO sorbent in the reactant mixture, the enhancement 'Enh' (in %) is calculated, defined by equation (9).

$$Enh = 100 \times \frac{\left(\text{Output with } CaO_{(S)} - \text{Output without } CaO_{(S)}\right)}{\text{Output without } CaO_{(S)}} \quad (9)$$

Equation (9) was used for comparisons of H_2 yield and purity in the results section.

2.4. Thermodynamic equilibrium calculations

Although the exact composition of the PEFB oil is unknown, the process of choosing the conditions for the steam reforming experiments was assisted by knowledge of the thermodynamic equilibrium for the reaction of its main components. Thermodynamic calculations for the steam reforming of acetic acid, levoglucosan, phenol, guaiacol, 2(5H) furanone, syringol, methyl guaiacol, eugenol, palmitic acid and methyl palmitate, which were identified as significant components of the bio-oils, were performed with and without the CO_2 sorbent $CaO_{(S)}$ in the reactant mixture. Thermodynamic properties have only recently

made available for such calculations, and those employed in here were compiled by Guenadou et al [41]. For calculations in the presence of CaO, two cases were considered, one where both the products of CaO hydration ($Ca(OH)_{2(S)}$), and of CaO carbonation ($CaCO_{3(S)}$) were included, and the other where $CaCO_{3(S)}$ was the only Ca-product allowed. This was to help discuss the profiles of the H_2 yield with temperature and molar steam to carbon ratio. The FORTRAN programme EQUIL [42] was used. It relies on a minimization of Gibbs free energy solution method. So as not to restrict the potential carbon products, 32 species in total were considered in the calculations such as stable C2- and C3- hydrocarbons and free radicals, but not solid carbon, whose thermodynamic properties when produced on catalysts are variable. The temperature range of 20-1000 °C was chosen to show the gradual effects of temperature on the different mechanisms contributing to hydrogen production. The calculations showed that the H-containing products reaching significant quantities (mol fractions exceeding 10^{-6}) were H_2, CH_4, and $Ca(OH)_{2(S)}$, and the main C-containing products were CH_4, CO_2, CO, $CaCO_{3(S)}$.

3. Results and discussion

3.1 Measured main compounds in the bio-oils

Tables 1 and 2 list the most significant organic compounds in the two bio-oils, identified by GC-MS using the NIST search library, alongside the percent surface area of their respective peaks. The compounds in Table 1 (PEFB) account for 75% of the total area of peaks recorded, and those in Table 2 (pine), 65%. Significant peaks of acetic acid were found both in the PEFB and pine oils at 32.06% and 15.17% respectively. Levoglucosan, the highest compound measured in pine oil at 28.11% was also detected in PEFB oil but at very low area percentage of 2.20%. Phenol, the second major compound detected for PEFB at 21.23% was not significant in pine oil (0.33%). Among other compounds measured in both oils were

syringol, guaiacol, 2(5H)-furanone, eugenol and methyl guaiacol, which are aromatic compounds. Small amounts of palmitic acid and methyl palmitate were also present.

3.2. Thermodynamic equilibrium of steam reforming of individual bio-oil compounds with and without CO_2 capture by CaO

3.2.1 Effects of temperature and S/C on acetic acid with and without CaO

The effects of steam to carbon ratio and temperature were investigated on the equilibrium H_2 yield from the steam reforming and the sorption enhanced steam reforming of the compound present in largest amounts and common to both the PEFB and pine bio oils, namely acetic acid. When ignoring thermodynamic equilibrium limitations, the reaction of steam reforming of acetic acid (below) can yield a maximum of or 13.3 wt% according to reaction 'SR-WGSac'

$CH_3COOH + 2H_2O \rightarrow 2CO_2 + 4H_2$ (SR-WGSac)

The H_2 yield versus temperature profiles are shown in Fig. 2 for increasing S/C ratios from 0 to 4. These profiles were calculated with the three Ca-species ($CaO_{(S)}$ reactant, $Ca(OH)_{2(S)}$ and $CaCO_{3(S)}$ products), simulating sorption enhanced steam reforming, and without any of the Ca-species, simulating conventional steam reforming. Additional profiles of H_2 yield obtained with CaO reactant and only $CaCO_3$ as the product are shown for just the S/C of 0.5 and 4 for the purpose of discussing the effects of hydration of $CaO_{(S)}$ during the sorption enhanced process. For conventional steam reforming, a similar pattern of curves was observed at S/C ratios above 0.5, in which the H_2 yield increased steeply between 200 and 580 °C (portion 'A'), peaked following a gradient that increased with increasing S/C (portion 'B'), and finally decayed with a shallow gradient rather independent on the S/C (portion 'C'). In the lowest temperature range (lower 'A'), the equilibrium product distribution (not shown) indicated a 50/50% split between CH_4 and CO_2 in the C- products, with CH_4 as the only H-

containing product, thus no net H_2 production was expected, independently of S/C. This can be seen as, in sequence, steam reforming of acetic acid into CO and $2H_2$, water gas shift, and methanation of CO (reverse steam methane reforming). With increasing temperature (mid 'A'), the equilibrium H_2 yield increased by the shift of methanation to steam methane reforming, but this was mitigated by the reverse water gas shift which also increased resulting in CH_4 still present as co-product. With further increases in temperature from ca. 600 to 700 °C (upper 'A'), steam methane reforming took over significantly over methanation, dominating the H_2 production against the reverse water gas shift reaction, and as a result the H_2 yield underwent a sharp increase. Above 700 °C, the reverse water gas shift was responsible for the slow, steady decay in H_2 yield ('B' and 'C'). The asymmetry between steep positive at low temperature and shallow negative gradients of H_2 yield at high temperature was caused by the stronger endothermicity of the steam reforming reactions (of acetic acid and methane) compared to the weak exothermicity of the water gas shift, and is common to steam reforming of hydrocarbons. According to Le Chatelier's principle, increasing the steam to carbon ratio results in a higher H_2 yield. The shift of the peak H_2 yield towards lower temperatures with S/C is a result of the stronger effect of S/C on the steam reforming reactions than on the water gas shift for temperatures below 600 °C, reflecting their different reaction enthalpies. At the stoichiometric S/C of 1, the equilibrium H_2 yield for steam reforming of acetic acid peaked at 707 °C with 68% H_2 eff (Eq.5), corresponding to 58% H_2 pur (Eq.3), whereas at the higher S/C of 4 the peak H_2 yield occurred at a lower 607 °C, with 89% H_2 eff and 64% H_2 pur. This illustrated the benefits of operating at higher S/C which result in higher H_2 yield and purity as well as lower temperature requirement. In practice, higher S/C represent higher costs of raising steam, with larger volumes of recycled water through the SR plant.

The presence of Ca-based sorption on the steam reforming of acetic acid is substantial. Using the Ca/C ratio of 1 corresponding to stoichiometry of the carbonation reaction, and allowing $CaCO_{3(S)}$ as the only Ca-product (Fig. 2), the profiles of high H_2 yield covered a much larger temperature range (from 0 to 700 °C) and reached significantly higher values than in the absence of $CaO_{(S)}$. A comparison of the H_2 yield and purity at S/C of 4 with and without $CaO_{(S)}$ illustrates well the triple benefit of sorption enhancement, namely, increasing the H_2 yield efficiency (from 89 to 98%), H_2 purity (from 64 to 98 %), and lowering the temperature of maximum H_2 yield (from 607 to 557 °C). The effects of the $CaO_{(S)}$ sorbent on the H_2 yield in the lower temperature range (A) were brought about by the shift in equilibrium in favour of the two hydrogen producing reactions (WGS and steam methane reforming), caused by the elimination of CO_2 from the syngas product, and decreasing the equilibrium concentration of CH_4. These would have simultaneously increased both H_2 yield and purity.

Accounting for the possibility of $Ca(OH)_2$ in addition to $CaCO_{3(S)}$ as the potential products of $CaO_{(S)}$ conversion had different effects according to S/C ratio and temperature (Fig. 2). In this case, the hydration reaction (‘Ca-HD’)

$$CaO_{(S)}+H_2O \leftrightarrow Ca(OH)_{2(S)} \qquad \text{Ca-HD}$$

was active at low to medium temperatures (up to 600 °C) and competed with CB for usage of $CaO_{(S)}$, and with SR as well as WGS for usage of H_2O, thus adversely shifting the equilibria of the three reactions. However, the removal of H_2O by $CaO_{(S)}$ would no longer be significant at the temperature of maximum H_2 yield, which occurs at around 600 °C, where the thermal decomposition of calcium hydroxide occurred (reverse Ca-HD), and $CaO_{(S)}$ was allowed again to convert exclusively to $CaCO_{3(S)}$ causing the desired sorption enhancement. In addition, the thermal decomposition of $Ca(OH)_2$ around and above 600 °C released H_2O thus favourably shifting SR and WGS, and causing further enhancement.

3.2.1. Effect of temperature for the other bio-oil compounds at S/C of 3.

Equilibrium H_2 yields were calculated at S/C of 3 with and without $CaO_{(S)}$ in the reactant mixture for most of the bio-oil compounds identified by GC-MS and listed in Tables 1 and 2 for the two oils (Fig. 3). A Ca/C ratio of 1 was used for the $CaO_{(S)}$ in the reactant mixtures, and both products $Ca(OH)_{2(S)}$ and $CaCO_{3(S)}$ were allowed in the equilibrium products. Similar profiles were obtained for these compounds than for acetic acid, reflecting the same chemical mechanism at work. All compounds exhibited significant sorption enhancement predicted by extending the region of high H_2 yield by ca. 200 °C towards lower temperatures, compared to conventional steam reforming. In all the cases, the temperature of maximum yield was shifted by more than 100 °C, and by yield enhancements (Enh, Eq.9) of between 14.7% (levoglucosan) and 16.5 % (2(5H) furanone) for the compounds of carbon atom of 10 and below. The lowest yield enhancement (12.7%) was calculated for palmitic acid and methyl palmitate.

3.3. Experiments of steam reforming without CO_2 sorbent: effect of steam to carbon ratio on reactants conversions, H_2 yield and selectivity to carbon products

The main process outputs for the steam reforming of both oils are presented in Table 3 for increasing S/C ratio at 600 °C. There are two S/C entries per row, one on the basis of the filtered oil with its natural water content ('wet S/C'), and the other on the basis of the moisture free (m.f.) oil. No addition of water during the experiments resulted in S/C of 0.76 for m.f. PEFB oil, and 0.37 for m.f. pine oil.

Under these conditions of no steam addition, the PEFB oil and the pine oil conversion to CO, CO_2 and CH_4 were only 67% and 69 % respectively, and the calculated water conversions were '107%' and '157%'. Equation 2 shows how underestimating the fuel

conversion would have resulted in erroneously high steam conversion. It is expected that for the experiments without steam addition some volatiles would have escaped analysis, however, the H_2 yield calculation, which is based on non- volatiles measurements, would have been reliable. Without steam addition, the H_2 yield was 8.06 wt% of the m.f. PEFB oil (74% H_2 eff), and 7.6 wt% of the m.f. pine oil (45 % H_2 eff). The lower yield obtained for pine oil was caused by a high selectivity to CO (61%) and to CH_4 (10%) in addition to incomplete oil conversion. Generally, high selectivity to CO reflects poor efficiency of the water gas shift reaction (either from lack of steam, insufficient catalyst activity, or insufficient reaction time), or equilibrium conditions favouring the reverse water gas shift (high temperature). High selectivity to CH_4 reflects poor catalyst activity for steam methane reforming, or equilibrium conditions favouring its reverse (methanation of CO). In the pine oil experiment without steam, fuel conversion was significantly less than 100% at 600 °C, neither reverse water gas shift nor methanation would be expected to be dominant, thus the low H_2 yield was due to poor efficiency in both water gas shift and steam methane reforming. For pine oil, the stoichiometric m.f. S/C was 1.36, therefore the first two conditions (S/C=0.37 and 1.01) lacked sufficient water, hence poor efficiency of SR and WGS, explaining the high selectivity to CO.

As expected, the H_2 yield increased with S/C. The condition 'wet' S/C of 1.89 (2.65 m.f. PEFB, 2.26 m.f. pine) corresponded to the highest oil fractional conversions to the carbon products CO, CO_2 and CH_4 (0.89 and 0.97, respectively). The H_2 purity and H_2 yield with time on stream are plotted for these optimum conditions in Figs. 4a-b and 5a-b for the PEFB oil and the pine oil respectively. In the case of PEFB oil, selectivity to CH_4 was low for the whole S/C range tested, with values below 5%, which in addition to good oil and water conversions, contributed to H_2 eff between 81 and 90% (Table 3). It is worth noting due to thermodynamic equilibrium limitations of the experiments without sorbent, as illustrated by

the calculations for acetic acid, 100% yield would be impossible. With increasing S/C, pine oil continued exhibiting high selectivity to CH_4 whereas selectivity to CO remained constant once the stoichiometric S/C of 1.36 had been exceeded (Table 3). Consequently, the 'wet' S/C of 2 was chosen to test the sorption enhancement effect by in-situ CO_2 capture using a CaO-based CO_2 sorbent in the steam reforming of both oils.

3.4. Carbon balance and catalyst characterization following steam reforming without sorption enhancement

Carbon balances for each experiment of steam reforming of PEFB and pine oils are listed in Table 4. This includes the amounts of carbon input as fuel to the reactor during fuel feeds, the carbon converted during fuel feed. The difference between these two amounts yielded carbon assumed deposited on the catalyst. This was followed by the carbon subsequently burnt off during the nitrogen and air feeds. The carbon balance (assumed deposited minus burnt-off) is indicated in the last column as a percent of the total carbon feed. As an average over the experiments with the two oils -to the exception of those without added steam, the carbon balances averaged 4.4% with a standard deviation of 5%. This may have been caused by either error propagations in the carbon balance calculations, or by a real effect of carbon residue on the catalyst.

The catalyst samples used in the PEFB and pine oil experiments were characterized by BET, XRD, SEM and TEM-EDX after the steam reforming experiments without sorbent. The TEM-EDX of catalysts after reforming both oils exhibited negligible amounts of carbon but significant amounts of Ni and O. For the PEFB oil, the EDX of the used catalyst also revealed very small amounts of calcium and silicon which would have originated from the oil's small impurities (0.05 wt% and 0.052 wt% respectively), as measured by ICP-MS. The

particles observed on the TEM images were approximately 50 nm in size. The XRD of the catalysts identified Al_2O_3, and NiO as the only phases present, with the Rietveld refinement yielding the composition 83.7% Al_2O_3, 16.3% NiO and 0% Ni for the catalyst used with PEFB oil, and 83.4 %,15.5% NiO and 1.1% Ni for the catalyst used with pine oil. For the used catalyst with PEFB oil, this represented just a slight deviation from the expected nominal 18 wt% NiO/Al_2O_3 composition of the as-received catalyst, and probably results from experimental uncertainties. For the used catalyst with pine oil, the measured 1.1% Ni indicates the oxidation at the end of the air feed was nearly complete. The XRD spectrum and its calculated profile with Rietveld refinement are shown in Fig. 6 for the pine oil experiment. In this figure, the residual curve defined by the difference between observed and calculated spectra can be seen to be close to zero. Both phase composition and crystallite sizes can be derived from these data. The Scherrer equation algorithm (corrected for peak broadening caused by instrumentation and strain), yielded a NiO crystallite size of 50.7 nm for the catalyst used with PEFB oil, and 45.5 nm for the catalyst used with pine oil, which are both close to that measured from XRD of the as-received catalyst (44.7 nm, Table 5). Two BET surface area analyses were carried out on the catalyst after steam reforming without sorbent, and surface areas of 2.2 and 2.8 $m^2\ g^{-1}$ were obtained for the catalyst used with PEFB oil, and of 3.2 and 2.6 $m^2\ g^{-1}$ for the catalyst used with pine oil. This was not significantly different from the as-received catalyst (3.2 and 2.6 $m^2\ g^{-1}$). Based on the relatively unchanged crystallite sizes and surface areas between the as-received and used catalyst, it could be concluded the catalyst had not undergone significant sintering, while the EDX and carbon balance indicated no obvious signs of deactivation by carbon deposition following air feed as a regeneration step. The solids characterization values are summarised in Table 5.

3.5. Steam reforming with Ca-based CO_2 sorbent at 600 °C and 'wet' S/C of 2

The average mol fractions from steam reforming experiments with steam activated calcined dolomite are presented in Table 6 on a dry mol basis for the wet S/C of 2 for both oils. The hydrogen purity and yield with time on stream are shown in Figs 4a-b and Fig. 5a-b alongside those obtained without sorbent. The experiments with the sorbent resulted in a higher H_2 yield (pre-sorbent saturation) than the experiments without sorbent. Pre-saturation conditions were measured for nearly 1 h operation. In pre-saturation conditions for both oils, the concentration of CO_2 in the gas products was small (below 1%), indicating the calcined dolomite was efficiently capturing CO_2 via the carbonation reaction. The concentrations of undesirable products such as CH_4 and CO were negligible during sorption: below 0.55 mol % for CH_4 and CO respectively. The lack of CO_2 and also lower CO and CH_4 in the products resulted in high purity of H_2, and demonstrated that the reaction equilibrium of WGS had shifted forward producing more hydrogen. Even though neither fuel nor steam conversions could be derived during sorption from elemental balances using the dry gas composition due to the unknown exact rate of CO_2 captured as carbonate, the closeness of the H_2 yield to its theoretical value strongly suggested that both had been very near their maxima. Quantification of the sorption enhancement effects on the H_2 yield and purity, shown in Table 6, indicated 9% and 41% enhancements in H_2 yield, and 67 % and 60% enhancements in H_2 purity for the PEFB and pine oils, respectively, compared to the values obtained without sorbent. Figures 4 and 5 show the enhancement effects were constant and sustained for at least 3500 s. For the calcined dolomite to be fully saturated, approximately 206 min with complete conversion of the oil to CO_2 and complete CO_2 capture would have been required. But the H_2 yields were seen to decrease beyond one hour operation, corresponding to ca. 30% sorbent use, despite maintaining a product of nearly pure hydrogen. This would have been caused by a gradual erosion of the steam reforming efficiency by carbon deposition while carbonation remained effective. A burn-off step under air feed achieved complete removal of

the carbon and regeneration of the sorbent by calcination, as shown by the absence of C, and the presence of the Ni, Al and O of the catalyst, with the Mg, Ca and O of the calcined dolomite in the relevant EDX spectrum (bottom right of Fig. 7). Whereas process efficiency under many cycles of sorbent carbonation and calcination remains to be investigated, the present study has demonstrated the beneficial effects of sorption enhancement on the steam reforming of PEFB and pine oils.

4. Conclusion

The effects of sorption enhancement, namely, substantial increases in both hydrogen yield and hydrogen purity of syngas, as well as a significant drop in the temperature of maximum H_2 yield, were demonstrated for the bio-oil model compound acetic acid and the $CaO_{(S)}$ sorbent using equilibrium calculations. The role played by the intermediate product calcium hydroxide ($Ca(OH)_{2(S)}$) was analysed in the equilibrium system. It showed the importance of operating at around 600 °C to prevent $Ca(OH)_2$ formation from decreasing the availability of $CaO_{(S)}$ for carbonation and of H_2O for steam reforming and water gas shift. Near full sorption-enhancement effects during steam reforming experiments were observed at 600 °C with PEFB oil, and significant enhancement was found for pine oil. This was achieved in the presence of steam-activated calcined natural dolomite and a Ni-based catalyst at the 'wet' molar steam to carbon ratio of 2 at atmospheric pressure. For PEFB oil, H_2 of purity above 96 vol% and H_2 yield approaching 10.4 wt% of the fuel, i.e. 95% of the maximum, were maintained for 42 min with the dolomite sorbent, compared to a H_2 purity of 67 vol% and yield of 9.51 wt% without sorbent. This represented enhancement effects of 67% and 9% in purity and yield, respectively. For pine oil, the H_2 purity and H_2 yield reached 87% and 13.9 wt% for 58 min respectively, representing 60% and 41% enhancement effects.

Acknowledgments

Our thanks to RCUK for grants EP/D078199/1 and EP/G01244X/1, Johnson Matthey for donation of catalyst materials, WBB Minerals for the dolomite from Warmsworth quarry and SIRIM Berhad/MOSTI, Malaysia for the scholarship for PhD student Mrs Rohaya Md Zin. We would like to also thank Dr Nicole Hondow for help with the electron microscopy work, and Professor Jenny M. Jones with Dr Andy B. Ross for use of their GC-MS and Karl Fischer titrator.

Nomenclature

Ca-HD	Calcium oxide hydration reaction
CB	Carbonation of CaO reaction
Enh	Enhancement, % (Eq.9)
H_2 Yield	Hydrogen yield (mol H_2/mol H_2 from fuel) or wt% of fuel (Eq.4)
H_2 eff	Hydrogen yield efficiency (ratio experimental yield to theoretical maximum, Eq. 5)
H_2 pur	Hydrogen purity according to Eq. 3
m.f.	moisture free
PEFB	Palm empty fruit bunches
S/C	Molar steam to carbon ratio
Sel	Selectivity to relevant product.
SR	Steam reforming
WGS	Water gas shift

X_{oil} Conversion fraction of pyrolysis oil (Eq. 1)

X_{H2O} Conversion fraction of water for experiments (Eq. 2)

References

1. Wang D, Montane D, and Chornet E. Catalytic steam reforming of biomass-derived oxygenates: Acetic acid and hydroxyacetaldehyde. Applied Catalysis A-General 1996; 143(2): 245-70.
2. Wang DN, Czernik S, and Chornet E. Production of hydrogen from biomass by catalytic steam reforming of fast pyrolysis oils. Energy & Fuels 1998; 12(1): 19-24.
3. Garcia L, French R, Czernik S, and Chornet E. Catalytic steam reforming of bio-oils for the production of hydrogen: effects of catalyst composition. Applied Catalysis A-General 2000; 201(2): 225-39.
4. Medrano JA, Oliva M, Ruiz J, Garcia L, and Arauzo J. Hydrogen from aqueous fraction of biomass pyrolysis liquids by catalytic steam reforming in fluidized bed. Energy 2011; 36(4): 2215-24.
5. Medrano JA, Oliva M, Ruiz J, Garcia L, and Afauzo J. Catalytic steam reforming of model compounds of biomass pyrolysis liquids in fluidized bed reactor with modified Ni/Al catalysts. Journal of Analytical and Applied Pyrolysis 2009; 85(1-2): 214-25.
6. Kechagiopouos PN, Voutetakis SS, Lemonidou AA, and Vasalos IA. Hydrogen Production via Reforming of the Aqueous Phase of Bio-Oil over Ni/Olivine Catalysts in a Spouted Bed Reactor. Industrial & Engineering Chemistry Research 2009; 48(3): 1400-8.
7. Vagia EC and Lemonidou AA. Hydrogen production via steam reforming of bio-oil components over calcium aluminate supported nickel and noble metal catalysts. Applied Catalysis a-General 2008; 351(1): 111-21.
8. Kechagiopoulos PN, Voutetakis SS, Lemonidou AA, and Vasalos IA. Sustainable hydrogen production via reforming of ethylene glycol using a novel spouted bed reactor. Catalysis Today 2007; 127(1-4): 246-55.
9. Dielbold JP, *A Review of the Chemical and Physical Mechanisms of the Storage Stability of Fast Pyrolysis Bio-Oils*. 2000, Thermalchemie, Inc, National Renewable Energy Laboratory (NREL): Colorado.
10. Basagiannis AC and Verykios XE. Influence of the carrier on steam reforming of acetic acid over Ru-based catalysts. Applied Catalysis B-Environmental 2008; 82(1-2): 77-88.
11. Basagiannis AC and Verykios XE. Catalytic steam reforming of acetic acid for hydrogen production. International Journal of Hydrogen Energy 2007; 32(15): 3343-55.
12. Basagiannis AC and Verykios XE. Reforming reactions of acetic acid on nickel catalysts over a wide temperature range. Applied Catalysis A-General 2006; 308: 182-93.
13. Bimbela F, Oliva M, Ruiz J, Garcia L, and Arauzo J. Hydrogen production by catalytic steam reforming of acetic acid, a model compound of biomass pyrolysis liquids. Journal of Analytical and Applied Pyrolysis 2007; 79(1-2): 112-20.
14. Takanabe K, Aika K, Seshan K, and Lefferts L. Sustainable hydrogen from bio-oil - Steam reforming of acetic acid as a model oxygenate. Journal of Catalysis 2004; 227(1): 101-8.

15. Takanabe K, Aika K, Seshan K, and Lefferts L. Catalyst deactivation during steam reforming of acetic acid over Pt/ZrO2. Chemical Engineering Journal 2006; 120(1-2): 133-7.
16. Wu C, Sui M, and Yan YJ. A Comparison of Steam Reforming of Two Model Bio-Oil Fractions. Chemical Engineering & Technology 2008; 31(12): 1748-53.
17. Kechagiopoulos PN, Voutetakis SS, Lemonidou AA, and Vasalos IA. Hydrogen production via steam reforming of the aqueous phase of bio-oil in a fixed bed reactor. Energy & Fuels 2006; 20(5): 2155-63.
18. Xu Q, Lan P, Zhang B, Ren Z, and Yan Y. Hydrogen Production via Catalytic Steam Reforming of Fast Pyrolysis Bio-oil in a Fluidized-Bed Reactor. Energy & Fuels 2010; 24(12): 6456-62.
19. Marquevich M, Czernik S, Chornet E, and Montane D. Hydrogen from biomass: Steam reforming of model compounds of fast-pyrolysis oil. Energy & Fuels 1999; 13(6): 1160-6.
20. Czernik S, French R, Feik C, and Chornet E. Hydrogen by catalytic steam reforming of liquid byproducts from biomass thermoconversion processes. Industrial & Engineering Chemistry Research 2002; 41(17): 4209-15.
21. Wang ZX, Pan Y, Dong T, Zhu XF, Kan T, Yuan LX, Torimoto Y, Sadakata M, and Li QX. Production of hydrogen from catalytic steam reforming of bio-oil using C12A7-O--based catalysts. Applied Catalysis A-General 2007; 320: 24-34.
22. Lea-Langton A, Md Zin R, Dupont V, and Twigg MV. Biomass pyrolysis oils for hydrogen production using chemical looping reforming. International Journal of Hydrogen Energy 2012; 37: 2037-43.
23. Shuit SH, Tan KT, Lee KT, and Kamaruddin AH. Oil palm biomass as a sustainable energy source: A Malaysian case study. Energy 2009; 34(9): 1225-35.
24. Sumathi S, Chai SP, and Mohamed AR. Utilization of oil palm as a source of renewable energy in Malaysia. Renewable & Sustainable Energy Reviews 2008; 12(9): 2404-21.
25. Sulaiman F, Abdullah N, Gerhauser H, and Shariff A. An outlook of Malaysian energy, oil palm industry and its utilization of wastes as useful resources. Biomass and Bioenergy 2011; 35(9): 3775-86.
26. Ridler DE and Twigg MV, *Steam reforming*, in *Catalyst Handbook*, M.V. Twigg, Editor. 1989, Wolfe Publishing Ltd: Frome, England. p. 225-80.
27. McCusker LB, Dreele RBV, Cox DE, Louer D, and Scardi P. Rietveld refinement guidelines. International Union of Crystallography 1999; 32(1): 36-50.
28. Dupont V, Ross AB, Knight E, Hanley I, and Twigg MV. Production of hydrogen by unmixed steam reforming of methane. Chemical Engineering Science 2008; 63: 2966-79.
29. Chrissafis K, Dagounaki C, and Paraskevopoulos KM. The effects of procedural variables on the maximum capture efficiency of CO2 using a carbonation/calcination cycle of carbonate rocks Thermochimica Acta 2005; 428: 193-8.
30. Dobner S, Sterns L, Graff RA, and Squires AM. Cyclic Calcination and Recarbonation of Calcined Dolomite. Industrial & Engineering Chemistry Process Design and Development 1977; 16(4): 479-86.
31. Balasubramanian B, Lopez Ortiz A, Kaytakoglu S, and Harrison DP. Hydrogen from methane in a single-step process. Chemical Engineering Science 1999; 54(15-16): 3543-52.
32. Silaban A, Narcida M, and Harrison DP. Characteristics of the reversible reaction between CO2(g) and calcined dolomite. Chemical Engineering Communications 1996; 146: 149-62.

33. Johnsen K, Ryu HJ, Grace JR, and Lim CJ. Sorption-enhanced steam reforming of methane in a fluidized bed reactor with dolomite as -acceptor. Chemical Engineering Science 2006; 61(4): 1195-202.
34. Hildenbrand N, Readman J, Dahl IM, and Blom R. Sorbent enhanced steam reforming (SESR) of methane using dolomite as internal carbon dioxide absorbent: Limitations due to $Ca(OH)_2$ formation. Applied Catalysis A: General 2006; 303(1): 131-7.
35. Han C and Harrison DP. Multicycle Performance of a Single-Step Process for H2 Production. Separation Science and Technology 1997; 32(1-4): 681-97.
36. Lopez Ortiz A and Harrison DP. Hydrogen Production Using Sorption-Enhanced Reaction. Industrial & Engineering Chemistry Research 2001; 40(23): 5102-9.
37. Dou BL, Dupont V, Rickett G, Blakeman N, Williams PT, Chen HS, Ding YL, and Ghadiri M. Hydrogen production by sorption-enhanced steam reforming of glycerol. Bioresource Technology 2009; 100(14): 3540-7.
38. Pimenidou P, Rickett GL, Dupont V, and Twigg MV. High purity H2 by sorption-enhanced chemical looping reforming of waste cooking oil in packed bed reactor Bioresource Technology 2010; 10(23): 9279-86.
39. Dou BL, Rickett GL, Dupont V, Williams PT, Chen HS, Ding YL, and Ghadiri M. Steam reforming of crude glycerol with in situ CO2 sorption. Bioresource Technology 2010; 101(7): 2436-42.
40. Pimenidou P, Rickett GL, and Dupont V, *In-situ CO2 capture for unmixed steam reforming*, in *8th World Congress of Chemical Engineering*. 2009: Montreal, Quebec, Canada.
41. Guenadou D, Lorcet H, Peybernes J, Catoire L, Osmont A, and Gokalp I. Plasma thermal conversion of bio-oil for hydrogen production. International Journal of Energy Research 2011; Published online.
42. Kee RJ, Rupley FM, Miller JA, Coltrin ME, Grcar JF, Meeks E, Moffat HK, Lutz AE, Dixon-Lewis G, Smooke MD, Warnatz J, Evans GH, Larson RS, Mitchell RE, Petzold LR, Reynolds WC, Caracotsios M, Stewart WE, and Glarborg P, *CHEMKIN Collection, Release 3.5, Reaction Design, Inc.,San Diego, CA, 1999*

Table 1 Main compounds detected by GC-MS for PEFB oil

Compounds	Area percentage
Acetic acid	32.06
Propanoic acid	0.89
1-Hydroxy-2-butanone	2.98
2(5H)-Furanone	0.28
2-Cyclopenten-1-one, 2-hydroxy-3-methyl-	8.34
Phenol	21.23
Phenol, 2-methoxy- (guaiacol)	1.99
Phenol, 2-methoxy-4-methyl (methyl guaiacol)	0.38
Phenol, 2,6-dimethoxy- (syringol)	4.60
Levoglucosan	2.20
	Total 74.95%

Table 2 Main compounds detected by GC-MS for pine oil

Compounds	Area percentage
Acetic acid	15.17
2(5H)-furanone	2.15
1,2-cyclopentanedione,3-methyl	3.94
Phenol	0.33
Phenol, 2-methoxy (guaiacol)	4.89
Phenol, 2-methoxy -4-methyl (methyl guaiacol)	5.44
Eugenol	1.70
Phenol, 2,6-dimethoxy- (syringol)	1.09
Vanillin	1.79
Levoglucosan	28.11
	Total 64.61%

Table 3 Process outputs for steam reforming of PEFB and pine oils with molar steam to carbon ratio at 600 °C in the absence of CO_2 sorbent. (max theor. H_2 yields are 10.9 and 17.1 wt% of moisture free PEFB and pine oils, respectively).

wet	m.f.	Conversions			% selectivity to C-products			Wt%mf	H_2 yield
		exp. theor.	exp.	max.					
S/C	S/C	X_{EFB}	X_{H2O}	X_{H2O}	$SelCO_2$	SelCO	$SelCH_4$	H_2 yield	eff.
PEFB									
0	0.76	0.67	1.07	1.00	47	51	2	8.06	0.74
0.64	1.43	0.77	0.63	0.72	51	45	4	8.72	0.81
1.22	1.98	0.83	0.45	0.51	42	53	5	8.88	0.82
1.89	2.65	0.89	0.36	0.38	43	55	2	9.50	0.87
2.00	2.75	0.87	0.34	0.37	39	59	2	9.51	0.87
2.52	3.28	0.83	0.31	0.31	53	42	5	9.73	0.90
Pine									
0	0.37	0.69	1.57	1.00	29	61	10	7.6	0.45
0.64	1.01	0.74	0.55	1.00	29	63	8	7.8	0.46
1.22	1.59	0.95	0.49	0.85	40	53	7	10.6	0.63
1.89	2.26	0.97	0.34	0.60	42	47	11	9.9	0.58
2.52	2.89	0.80	0.35	0.47	52	42	6	12.2	0.72

Table 4 Carbon balance PEFB and pine oils without sorbent, based on total mol of C input minus mol of C converted (to CO, CO_2 and CH_4) during the fuel feed, minus the mol of C subsequently oxidised during both air and N_2 feeds.

wet S/C feed→	mol C in Fuel/H_2O	mol C conv Fuel/H_2O	mol C oxid Air	mol C oxid N_2	mol C oxid Air & N_2	C bal (mol)	C bal (%)
PEFB							
0.00	2.26×10^{-2}	1.52×10^{-2}	3.22×10^{-3}	2.42×10^{-4}	3.46×10^{-3}	3.89×10^{-3}	17.2
0.66	3.18×10^{-2}	2.44×10^{-2}	5.58×10^{-3}	2.86×10^{-4}	5.87×10^{-3}	1.51×10^{-3}	4.8
1.23	2.98×10^{-2}	2.47×10^{-2}	3.29×10^{-3}	6.07×10^{-6}	3.29×10^{-3}	1.84×10^{-3}	6.2
1.89	3.26×10^{-2}	2.70×10^{-2}	4.17×10^{-3}	2.83×10^{-7}	4.17×10^{-3}	1.43×10^{-3}	4.4
2.51	3.26×10^{-2}	2.70×10^{-2}	3.07×10^{-3}	7.80×10^{-5}	3.15×10^{-3}	2.48×10^{-3}	7.6
Pine							
0	2.25×10^{-2}	1.59×10^{-2}	N.A.	N.A.	N.A.	N.A.	N.A.
0.66	3.29×10^{-2}	2.43×10^{-2}	8.25×10^{-3}	2.33×10^{-4}	8.48×10^{-3}	1.19×10^{-4}	0.4
1.23	5.16×10^{-2}	4.90×10^{-2}	3.23×10^{-3}	1.32×10^{-3}	4.55×10^{-3}	2.02×10^{-3}	3.9
1.89	1.96×10^{-2}	1.90×10^{-2}	N.A	N.A.	N.A.	N.A.	N.A.
2.51	2.20×10^{-2}	1.75×10^{-2}	1.92×10^{-3}	2.13×10^{-5}	1.94×10^{-3}	2.54×10^{-3}	11.5

Table 5 Characterisation of the catalyst by N_2 adsorption (BET surface area) and powder XRD (composition and crystallite size)

Sample	Conditions	BET (m^2g^{-1})	Al_2O_3 (wt%)	NiO (wt%)	Ni (wt%)	NiO crystallite size (Å)
As-received	oxide	3.262 1.884	n.a	n.a	n.a	447
Reduced	H_2 reduced	3.720 2.798	n.a	n.a	n.a	n.a
Used	PEFB, after air feed	2.819 2.203	83.7	16.3	0	506.6
Used	Pine, after air feed	3.258 2.557	83.4	15.5	1.1	455.5

Table 6 Process outputs of sorption enhanced steam reforming of PEFB and pine oils at wet S/C of 2 (PEFB) and 1.9 (pine) and 600 °C. The enhancement effect given in % change, compared to the values without sorption are also shown in brackets.

Oil	duration (s)	H_2 yield (wt% of fuel)	H_2 purity (%)	Concentrations (Mol %)			
				CO_2	CO	CH_4	H_2
PEFB	2500	10.4 (Enh+9%)	97 (Enh+67%)	0.007	0.11	0.03	5.12
Pine	3500	13.9 (Enh+41%)	87 (Enh+60%)	0.66	0.55	0.21	9.92

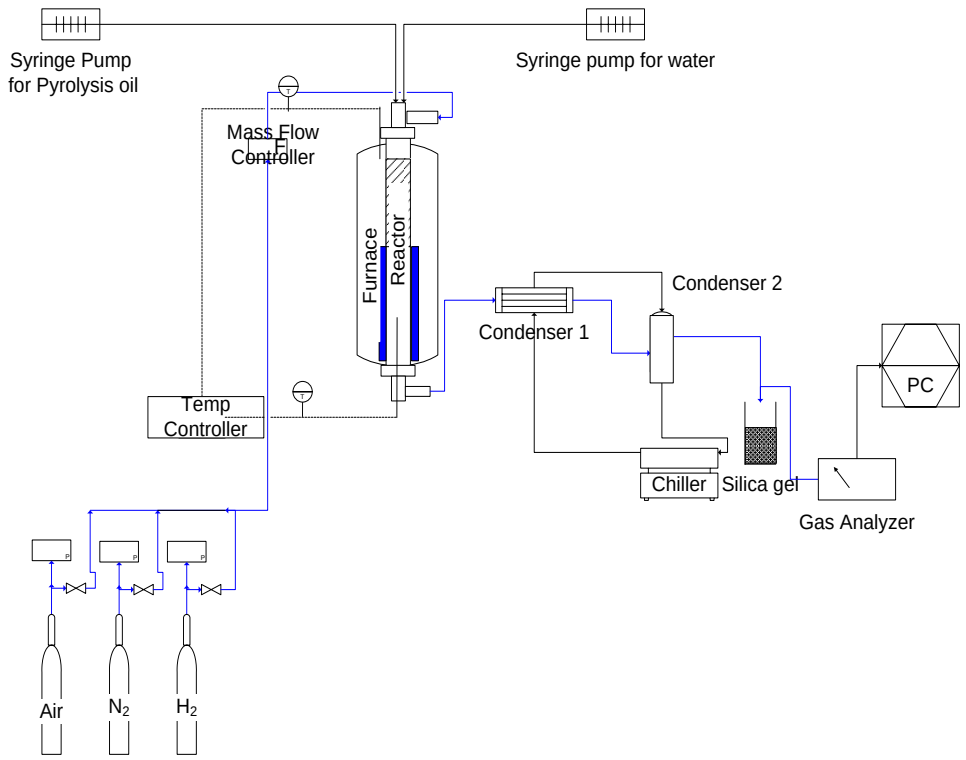

Fig. 1 Experimental set-up for the steam reforming of the pyrolysis oils.

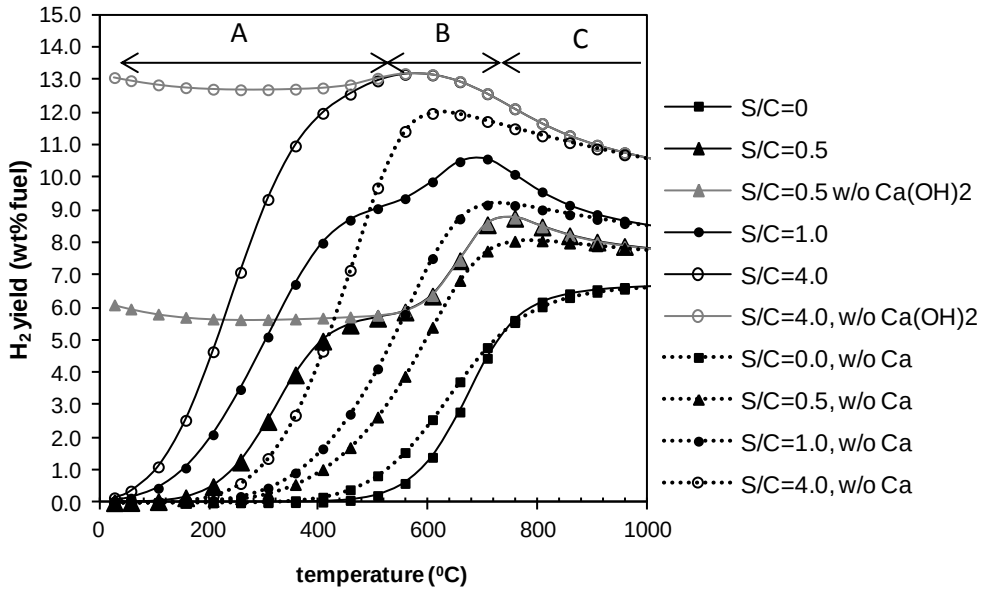

Fig. 2 H_2 yield from acetic acid at thermodynamic equilibrium vs. temperature at different S/C ratios (0-4). 'w/o Ca', dotted lines represent reactant mixtures without $CaO_{(S)}$; solid black lines: reactant mixtures with $CaO_{(S)}$ at molar Ca/C ratio of 1, allowing both $CaCO_{3(S)}$ and $Ca(OH)_2$ products; 'w/o $Ca(OH)_2$', solid grey lines: as black lines but allowing $CaCO_{3(S)}$ as the only Ca-product.

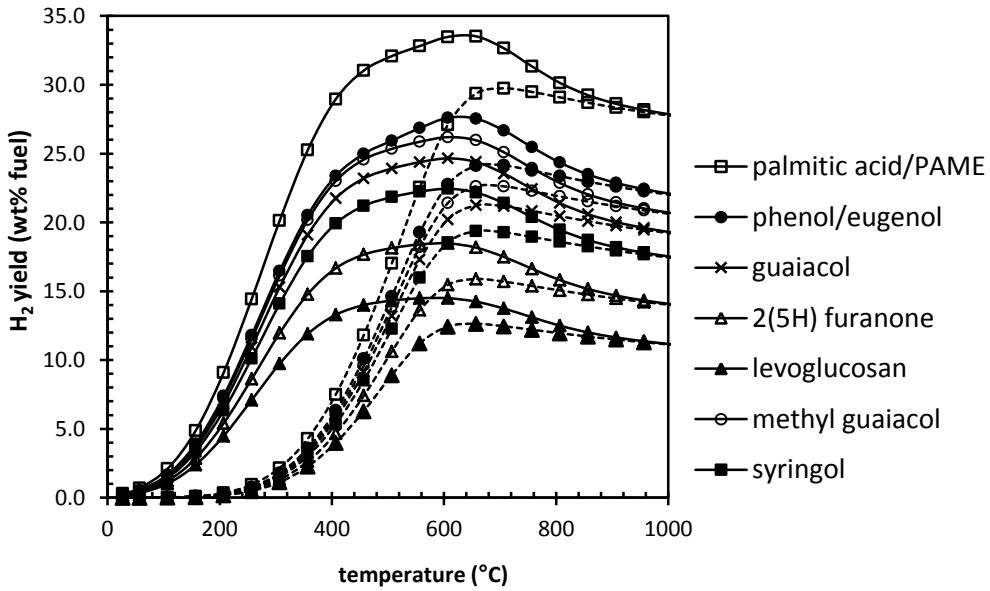

Fig. 3 H_2 yield for S/C of 3.0 for the bio-oil compounds measured in significant concentrations by GC-MS (Tables 1&2). Dotted lines represent reactant mixtures without CaO (conventional steam reforming), and solid lines represent reactant mixtures with CaO/C ratio of 1 (sorption enhanced steam reforming). The following substances produced nearly superimposed profiles: palmitic acid with methyl palmitate (PAME), phenol with eugenol.

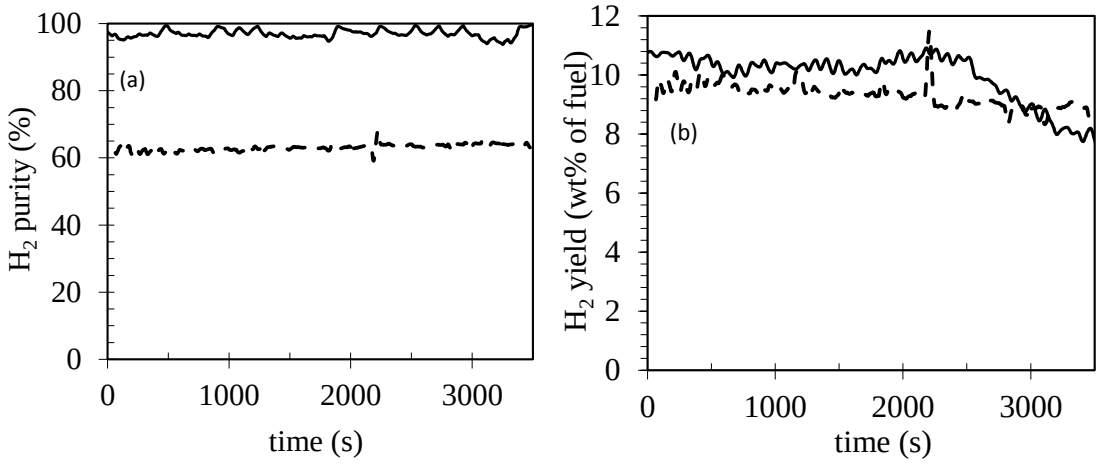

Fig. 4: (a) H_2 purity and (b) Yield of the hydrogen produced during steam reforming and sorption-enhanced steam reforming of PEFB pyrolysis oil 600 °C and S/C of 2.52.

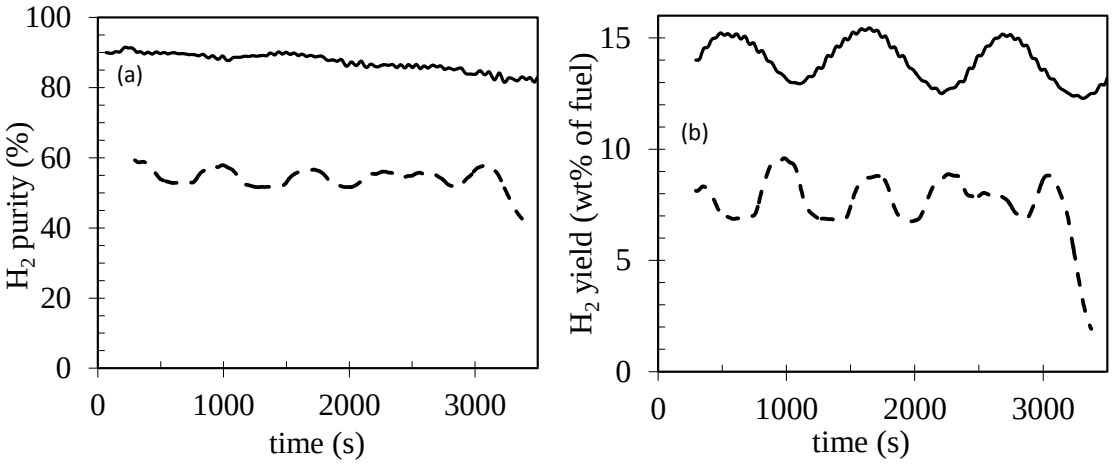

Fig. 5 as Fig. 4 for pine oil at S/C of 2.

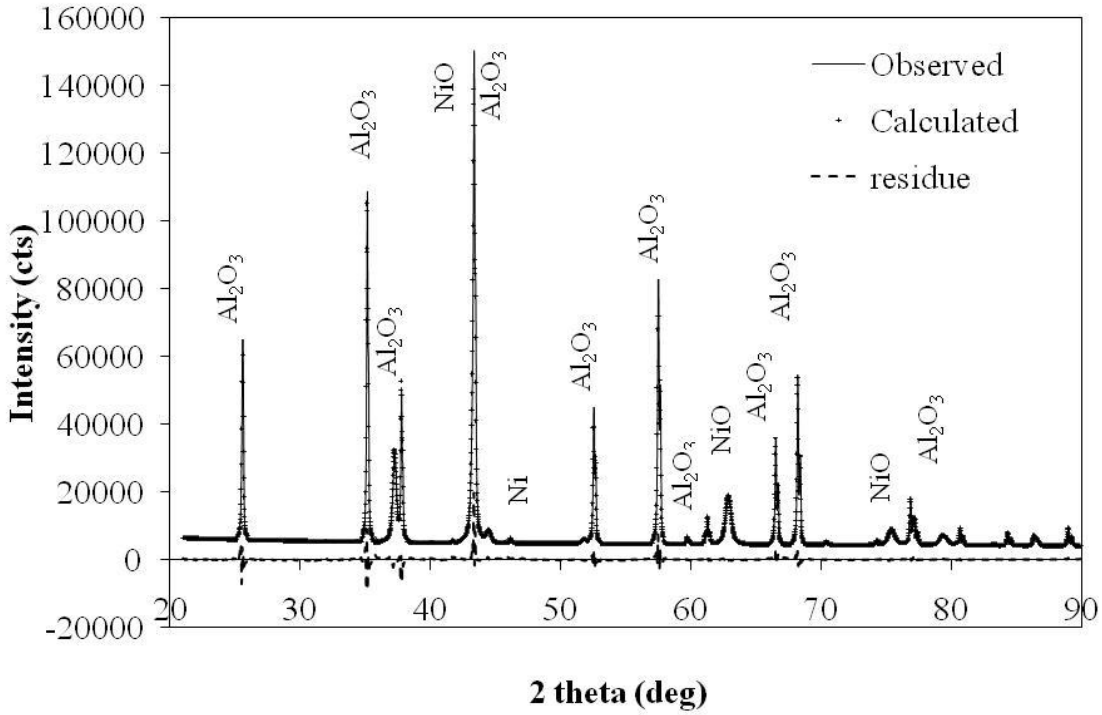

Fig. 6 XRD observed spectrum for pine oil after wet S/C=2 experiments without sorbent, following final air feed (solid line), also shown the calculated spectrum with Rietveld refinement (scatter points) and the residue line between the two spectra (dashed line).

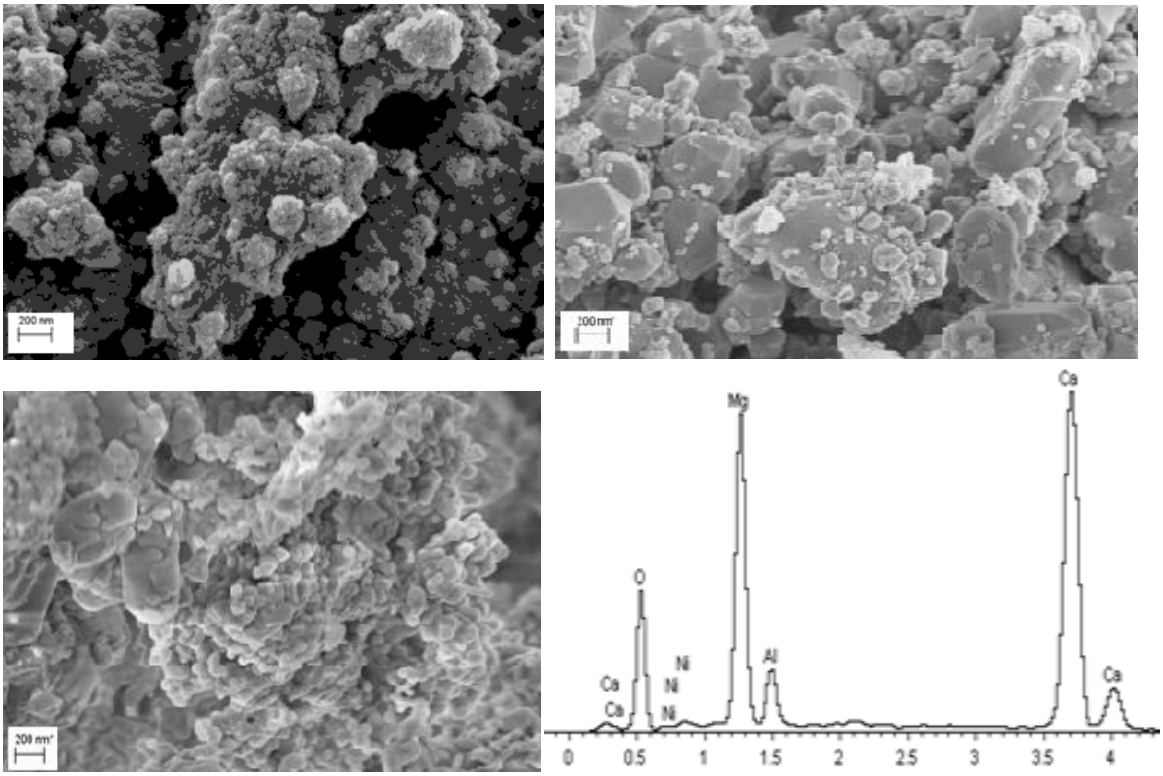

Fig. 7 SEM images for pine EPFB oil for wet S/C=2. Top left: experiment without sorbent after fuel and steam feed and N_2 purge, top right: same after the air feed, bottom left: with sorbent after air feed. Bottom right: EDX of SEM image in bottom left.